analytical chemistry

pubs.acs.org/ac
Article

Amplification-Free Attomolar Detection of Short Nucleic Acids with Upconversion Luminescence: Eliminating Nonspecific Binding by Hybridization Complex Transfer

Jakub Máčala,[§] Saara Kuusinen,[*,§] Satu Lahtinen, Hans H. Gorris, Petr Skládal, Zdeněk Farka, and Tero Soukka

Cite This: *Anal. Chem.* 2025, 97, 1775−1782
Read Online

ABSTRACT: The anti-Stokes emission of photon upconversion nanoparticles (UCNPs) facilitates their use as labels for ultrasensitive detection in biological samples as infrared excitation does not induce autofluorescence at visible wavelengths. The detection of extremely low-abundance analytes, however, remains challenging as it is impossible to completely avoid nonspecific binding of label conjugates. To overcome this limitation, we developed a novel hybridization complex transfer technique using UCNP labels to detect short nucleic acids directly without target amplification. The assay involves capturing the target−label complexes on an initial solid phase, then using releasing oligonucleotides to specifically elute only the target−UCNP complexes and recapturing them on another solid phase. The nonspecifically adsorbed labels remain on the first solid phase, enabling background-free, ultrasensitive detection. When magnetic microparticles were used as the first solid phase in a sample volume of 120 μL, the assay achieved a limit of detection (LOD) of 310 aM, a 27-fold improvement over the reference assay without transfer. Moreover, the additional target-specific steps introduced in the complex transfer procedure improved the sequence specificity of the complex transfer assay compared with the reference assay. The suitability for clinical analysis was confirmed using spiked plasma samples, resulting in an LOD of 190 aM. By increasing the sample volume to 600 μL and using magnetic preconcentration, the LOD was improved to 46 aM. These results highlight the importance of background elimination in achieving ultralow LODs for the analysis of low-abundance biomarkers.

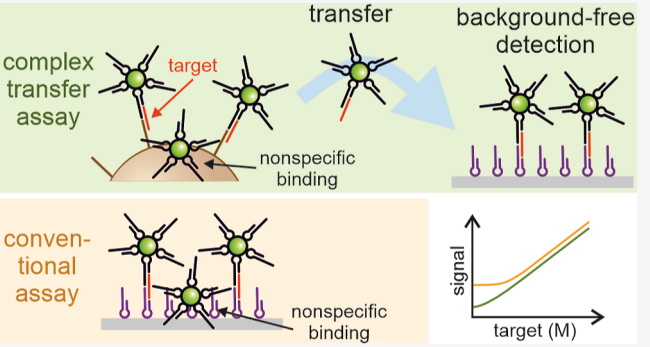

INTRODUCTION

Nucleic acid testing is an essential part of modern diagnostics, especially in the diagnostics of infectious diseases and cancer. A major part of nucleic acid testing is done by using quantitative polymerase chain reaction and other target amplification-based methods, as they generally reach the lowest limits of detection (LOD).[1] However, amplification-based methods are prone to false results upon contamination and amplification biases. Additionally, the quantitative detection of short targets, such as microRNAs (miRNA), is challenging, as the hybridization of short primers is not always efficient and reliable.[2] Furthermore, amplification-based methods typically require isolation of nucleic acids from the sample matrix to remove enzyme inhibitors, introducing an additional step and potential source of bias to the workflow.[3,4] On the other hand, amplification-free methods, such as Northern blot, in situ hybridization, next-generation sequencing, and microarrays, are designed to detect the target sequence directly.[5−7] However, their sensitivity is often not sufficient for diagnostic use.

Photon-upconversion nanoparticles (UCNPs) are a group of nanomaterials capable of a unique type of luminescence emission, anti-Stokes photoluminescence,[8] rendering them highly attractive labels for bioaffinity assays. The lanthanide-doped inorganic UCNPs (e.g., hexagonal $NaYF_4$:Yb^{3+}, Er^{3+}) can produce visible emission under infrared excitation due to the ladder-like long-lived energy states of the lanthanides and the capability to stack the energy of two or more sequentially absorbed photons.[9] As a result of the anti-Stokes emission, the autofluorescence of the biological sample matrix and solid-phase material can be completely eliminated. Therefore, biomarker detection and imaging can be carried out even in complex biological matrices without optical background interference.[10] Photostability and resistance to photobleaching

Received: October 7, 2024
Revised: December 9, 2024
Accepted: December 18, 2024
Published: January 12, 2025

under continuous excitation are other advantages of UCNPs over conventional labels, such as organic fluorophores.[11]

Due to their excellent properties as labels, UCNPs have also been used for nucleic acid detection. For example, Guan et al.[12] reported the amplification of miRNA using CRISPR/Cas13-based enzymes, which was then detected by magnetic UCNPs on a biosensor platform, achieving a limit of detection (LOD) of 83 fM. Wu et al.[13] detected two miRNA biomarkers for breast cancer simultaneously using green- and blue-emitting UCNPs as Förster resonance energy transfer (FRET) donors and MoS_2 nanosheets as FRET quenchers. The presence of miRNAs in the sample prevented FRET, resulting in LODs of 0.17 nM for miRNA-593 and 0.25 nM for miRNA-155. Chen et al.[14] employed UCNPs in a multimode lateral flow assay to detect miRNA via colorimetry, luminescence, and surface-enhanced Raman spectroscopy. This platform allowed miRNA detection in the concentration range from 1 fM to 2 nM. Wang et al.[15] reported the detection of circulating tumor DNA (ctDNA) based on FRET between UCNP-based donor probes and gold nanocages acting as energy acceptors, reaching an LOD of 6.3 pM.

While UCNPs are detectable without optical background interference, the background signal generated by nonspecific binding of label conjugates becomes the sensitivity-limiting factor. Variation of the nonspecific binding in the assays can also contribute to the inaccuracy, ultimately leading to falsely negative or positive results.[16,17] There are several ways to reduce the amount of nonspecifically bound labels, for example, using more effective washing procedures, thorough optimization of the composition and amount of the assay components, and efficient blocking of the detection surface.[18−20] However, excessive washing can decrease assay sensitivity by washing off even a substantial part of the specifically bound labels.[18] Target-dependent covalent ligation has been used to enable more stringent washing.[21] Another way of increasing the signal-to-background ratio is by promoting specific interactions. For example, the rate of specific hybridization can be increased by concentrating the target oligonucleotides by addition of crowding agents, such as poly(ethylene glycol).[22]

Another well-known way to improve the analytical sensitivity of bioaffinity assays is the digital readout, based on counting single labels bound to the solid-phase surface.[24] However, if the analytical sensitivity is limited by nonspecific binding, the digital readout does not necessarily improve the assay performance.[23] An alternative approach to increase the assay sensitivity is reducing the capture surface area to maximize the density of the specific binding, thus increasing the signal-to-background ratio by the so-called ambient analyte assays.[25]

For bioanalytical applications, surface modification is required to render UCNPs dispersible in aqueous solutions and enable conjugation with biomolecules. Surface coating with polymers, such as poly(ethylene glycol) or poly(acrylic acid), yields a protective layer and prevents the nonspecific binding of assay components to the particle surface.[23,26] Different surface modifications and conjugated biomolecules have different tendencies for nonspecific interactions with other biomolecules and biomolecule-coated surfaces.[23,27−29] Thus, each particular combination of surface chemistry and molecular recognition elements in the assay may require separate optimization.

Despite efforts to minimize nonspecific binding, it has been practically impossible to eliminate it completely. However, we introduce an assay principle for the detection of short nucleic acid sequences that overcomes this limitation by utilizing the hybridization complex transfer technique. The assay uses two consecutive target-specific capture steps, and the elimination of the nonspecific background signal is based on the specific release of the target sequences from the first capture probes by toehold-mediated strand displacement[30] with releasing oligonucleotides. As a result, only the target−UCNP complexes are released from the first capture probes and recaptured onto the second solid phase, while nonspecifically bound UCNPs remain on the first solid phase. Therefore, only specifically target-bound UCNPs are detected on the second solid phase, resulting in complete elimination of the assay background and ultrasensitive detection of the target. This type of complex transfer assay has not been reported before for the detection of nucleic acids. The assay principle is an improved version of the immunocomplex transfer assay originally developed by Kohno et al.[31,32] In their assay, the entire two-site immunocomplex, including the capture antibody, was released and recaptured. Therefore, the unoccupied capture antibodies were transferred, too. With nucleic acids, it is easier to release only the target−label complexes without releasing capture probes. This enables the use of a large surface area in the first capture step to enhance the binding kinetics, followed by the second capture step onto a smaller surface area to maximize the signal intensity on the readout area.[33] By using magnetic beads (MBs) as the solid phase, this also enables the preconcentration of the target from a larger sample volume, further improving the sensitivity of the assay. We used synthetic DNA oligonucleotide corresponding to the miR-20a sequence (DNA-miR-20a) as a model target in assay development to demonstrate the potential of the complex transfer assay technique while excluding possible stability issues of RNA.[34]

EXPERIMENTAL SECTION

Chemicals and Materials. Synthetic oligonucleotides (sequences listed in Table S1, Supporting Information) were obtained from Biomers (Germany). Kaivogen buffer solution (assay buffer), Kaivogen wash buffer, and white streptavidin-coated microtiter plates (MTP) were purchased from Uniogen Oy (Finland). Pierce 1 μm streptavidin MBs and Lumi Lockwell White Maxisorp 96-well MTPs were purchased from Thermo Fisher (USA). Streptavidin was obtained from IBA Life Sciences (Germany). Bovine serum albumin was obtained from Bioreba (Switzerland). Hybridization buffer and elution buffer were prepared by adding NaCl and KF to the assay buffer, resulting in 3.6 M NaCl and 5 mM KF in the hybridization buffer and 1 M NaCl and 1 mM KF in the elution buffer. Hybridization wash buffer was prepared by adding 0.3 M NaCl, 0.1% (w/v) Tween 20, and 1 mM KF to the wash buffer.

Information on the oligonucleotide design, protocols for synthesis, and surface modification of UCNPs ($NaYF_4$:Yb^{3+}, Er^{3+}) and their conjugation with tracer probes, as well as characterization of UCNPs and UCNP-tracer probe conjugate with transmission electron microscopy and dynamic light scattering (Figure S1), and information on the plasma pool collection and in-house coating of MTPs with streptavidin are provided in the Supporting Information.

Hybridization Complex Transfer Assay with Microtiter Wells as the First Capture Surface. MTPs for the first and second capture steps were coated with capture probes just before use. The wells of commercial streptavidin-coated 96-

https://doi.org/10.1021/acs.analchem.4c05401
Anal. Chem. 2025, 97, 1775−1782

well MTPs were prewashed with the wash buffer and coated with the biotinylated first capture probe by adding 150 μL of 50 nM probe dilution in assay buffer to each well and incubating the plate at room temperature under slow shaking for 30 min. For the second capture step, the biotinylated second capture probes were diluted to a final concentration of 50 nM in assay buffer supplemented with 5% ethanol, heated to 80 °C for 5 min to denature probe dimers, and cooled at room temperature. The in-house coated streptavidin MTP was prewashed with the wash buffer, and the biotinylated second capture probe was immobilized onto the bottom of the wells by incubating 25 μL of the probe per well for 30 min without shaking. The unbound probes were removed by washing the wells once with a wash buffer.

Calibrators were prepared by diluting target DNA oligonucleotides in 50 mM Tris-HCl, pH 7.75, 0.9% NaCl, 0.05% NaN_3 containing 7.5% bovine serum albumin. UCNP−DNA probe conjugates were diluted to a concentration of 75 μg/mL in hybridization buffer and bath-sonicated for 3 min. The UCNP conjugate dilution was mixed with samples or calibrators in a 20:80 volume ratio (resulting in 15 μg/mL UCNP conjugates, 0.85 M NaCl, and 1 mM KF in the hybridization reaction). The UCNP−target complexes were formed by incubating the hybridization reactions for 30 min at room temperature under slow rotation, after which 150 μL of hybridization reaction mixtures (corresponding to 30 μL of the UCNP conjugates in hybridization buffer and 120 μL of the sample) was pipetted to the first capture probe-coated wells. The complexes were captured by incubating the plate at room temperature under slow shaking for 1 h. The wells were washed four times with hybridization wash buffer, and 5 pmol releasing oligonucleotide was added to each well in 150 μL of elution buffer and incubated at room temperature under slow shaking for 45 min. The released target−UCNP complexes were transferred to the second capture wells (140 μL/well) and incubated for 90 min at room temperature under slow shaking. The wells were washed four times with the hybridization wash buffer and left to dry. Finally, the upconversion luminescence (UCL) was measured.

Hybridization Complex Transfer Assay Using MBs as the First Capture Surface. Complex transfer assay with MBs as the first capture surface was carried out as described for the MTP wells, with some modifications. Streptavidin-modified MBs were prewashed twice with wash buffer and coated with the biotinylated first capture probes (1 mg/mL beads, 100 nM first capture probes in assay buffer) for 60 min under 1200 rpm shaking. The capture probe-coated MBs were washed 3 times with wash buffer to remove unbound probes. Calibrators were prepared by diluting target DNA oligonucleotides in the assay buffer. The volume of samples or calibrators was either 120 or 600 μL per reaction, and the volume of the UCNP dilution was scaled accordingly (i.e., 30 or 150 μL per reaction, respectively). The UCNP−target complexes were formed as described for the MTP assay. To capture the complexes, a final concentration of 0.17 mg/mL MBs was added to the UCNP−target mixtures, and the reaction mixture was incubated in microtubes under 1200 rpm orbital shaking for 60 min at room temperature. Afterward, the MBs were washed four times with hybridization wash buffer, and the target−UCNP complexes were released by adding 0.1 nmol of releasing oligonucleotide per 1 mg of MBs in 40 μL/reaction in the elution buffer. The strand displacement reaction mixture was incubated for 30 min under 1200 rpm shaking. The MBs were removed from the reactions with a magnet, and 40 μL of the supernatant was transferred into each second capture well, prepared as described for the MTP assay. Thereafter, the wells were incubated for 30 min at room temperature under slow shaking to capture the UCNP−target complexes. After the wells were washed and dried, the UCL was measured.

UCL Readout and Data Evaluation. UCL at 540 nm was measured as an average of a 3 × 3 point raster (point-to-point distance 1.5 mm) measurement of 2 s readouts from the bottom of a microtiter well using a modified Chameleon plate reader (Hidex Oy, Finland) equipped with a 980 nm laser excitation source.[35] The standard curves were fitted with a 4-parameter logistic function in Origin 2016, and the LODs were calculated by adding three times the standard deviation of the zero calibrator to the average signal of the zero calibrator, followed by determining the corresponding concentration from the regression curve. The data evaluation and LOD determination are described in detail in the Supporting Information.

RESULTS AND DISCUSSION

The principle of the hybridization complex transfer assay is illustrated in Figure 1. The sample containing the target or calibrator DNA is first mixed with a hybridization buffer containing UCNPs conjugated with hairpin-structured DNA probes to form target−UCNP complexes (step I). The hairpin structures stabilize the hybridization via base-stacking interactions between adjacent bases.[36] The complexes are then captured using biotin-modified capture DNA probes immobilized on the first capture surface of either streptavidin-coated MTP wells or streptavidin-coated MBs (step II). After washing off the unbound reagents, releasing DNA oligonucleotides are added. The releasing oligonucleotides were designed to hybridize with the capture probes more strongly than the target, thus displacing the target−UCNP complexes via a toehold-mediated strand displacement reaction. The capture probes contain a toehold domain, which is located next to the target binding domain and is complementary to the releasing oligonucleotide. The partial hybridization of the releasing oligonucleotide to the toehold domain in the capture probe initiates the strand displacement reaction (step III). The releasing oligonucleotide then displaces the target sequence via branch migration and releases the target−UCNP complex into the solution. In contrast, UCNPs nonspecifically bound to the first capture surface are not released (step IV). The solution containing the released target−UCNP complexes is transferred to a fresh streptavidin-coated MTP modified with a biotinylated, hairpin-structured, and target-specific capture probe (step V). The target−UCNP complexes bind to the second capture probe, and after washing and drying, the UCL at 540 nm is measured from the bottom of the well upon 980 nm laser excitation (step VI).

The assay was first optimized using an MTP as a solid phase for both capture steps to find the optimal conditions for the hybridization of the target with capture probes as well as for releasing the target complex. The first capture of the target from the sample was carried out in commercial MTP wells completely coated with streptavidin. The second capture step was carried out in MTP where streptavidin was present only on the bottom of the wells to concentrate the UCNP−target complexes on the scanned area of the well to maximize the signal intensities. Figure S2 in the Supporting Information shows that 13 nucleotides were an optimal length for the

https://doi.org/10.1021/acs.analchem.4c05401
Anal. Chem. 2025, 97, 1775−1782

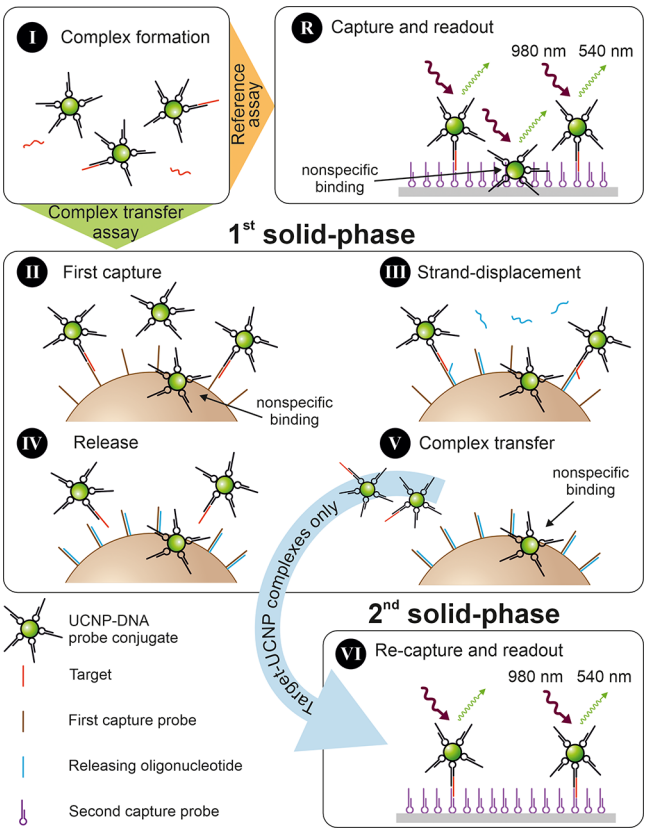

Figure 1. Principle of the hybridization complex transfer assay utilizing MBs as the first capture surface. (I) The sample is mixed with the UCNP−DNA probe conjugates to form target−UCNP complexes. (II) The complexes are captured with DNA probes immobilized on the surface of MBs. (III) The beads are washed, and releasing oligonucleotides are added. Releasing oligonucleotides hybridize with the capture probes, displacing the target via toehold-mediated strand displacement. (IV) Target−UCNP complexes are released into the solution, and (V) the solution is transferred into microtiter plate wells coated with another capture probe. (VI) The target−UCNP complexes are collected with the capture probes, the wells are washed and dried, and UCL is measured. In the reference assay (R), the complexes formed in the step (I) are directly captured onto wells coated with the second capture probes.

sequence in the releasing oligonucleotide binding to the toehold domain in the first capture probe. Figure S3 shows that the optimal elution buffer contained a minimum of 0.7 M NaCl. The complex transfer assay was performed in a sample volume of 120 μL per MTP well. In a reference assay, the UCNP−target complexes were formed in the same volume as in the complex transfer assay, but the complexes were captured directly onto the MTP solid phase used in the second capture step, i.e., without the first capture and complex transfer steps.

The standard curves of the hybridization complex transfer assay and the reference assay are presented in Figure 2. The complex transfer assay yielded an LOD of 0.66 fM, about 9-fold lower than the LOD of 5.7 fM obtained by the reference assay. Although the signal responses in the linear range obtained by the complex transfer assay were 48−56% lower compared to the reference assay, the background signal originating from nonspecifically bound labels (i.e., the signal of the zero calibrators after subtracting the instrument background) was reduced by more than 99%, thus being much more important to obtain the lowest possible LOD than

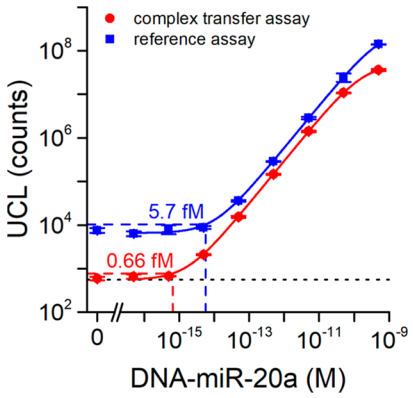

Figure 2. Standard curves of the complex transfer assay (red, circles) and the reference assay without complex transfer (blue, squares). Both captures of the complex transfer assay were carried out in an MTP. Dashed lines indicate the LODs, and the dotted line shows the instrument background. Error bars represent the standard deviations of three replicates (or six replicates in case of zero calibrators).

the overall luminescence signal. The signal of zero calibrators (595 ± 61 counts) was at the level of the instrumental background (555 ± 23 counts), which was now the limiting factor of the sensitivity of the complex transfer assay together with the binding and detectability of the labels[37] instead of the nonspecific binding. This confirmed the assumption that complex transfer and subsequent elimination of the background caused by nonspecifically bound labels would allow for achieving lower LODs.

To further improve the performance of the complex transfer assay, MTP was replaced by streptavidin-coated magnetic MBs as the first capture surface. The advantage of using MBs as a solid phase is their large surface area and the possibility of increasing the ratio of the capture surface area to the sample volume, thus increasing the concentration of capture probes and subsequently improving the capture kinetics. For the first capture step, the MBs were incubated for 1 h in a mixture containing 120 μL of the sample and 30 μL of UCNPs in the hybridization buffer. The binding kinetics of the UCNP−target complexes depended on the MB concentration, and the binding was slower when the MB concentration was reduced to 50% (Figure S4 in the Supporting Information).

In order to obtain the best possible performance of the complex transfer assay utilizing the MBs as the first capture surface, the UCNP label concentration, releasing oligonucleotide concentration, incubation times of the first capture on MBs and second capture on MTP, and the elution of the complexes from MBs were optimized (Figures S5 and S6 in the Supporting Information). Under optimal conditions, even though the signal responses in the complex transfer assay were 40−60% lower compared to the reference assay (Figure 3A), the hybridization complex transfer assay achieved an LOD of 0.31 fM (corresponding to approximately 22,000 target DNA molecules), improving the LOD by a factor of 27, compared to the reference assay with an LOD of 8.3 fM (corresponding to 600,000 target DNA molecules).

To demonstrate that the complex transfer assay is suitable for detecting the target directly from plasma samples, EDTA plasma pool aliquots were spiked with known target concentrations and analyzed by the complex transfer assay, utilizing MBs as the first capture surface and by the reference assay. The LOD in EDTA plasma was 0.19 fM (14,000

https://doi.org/10.1021/acs.analchem.4c05401
Anal. Chem. 2025, 97, 1775−1782

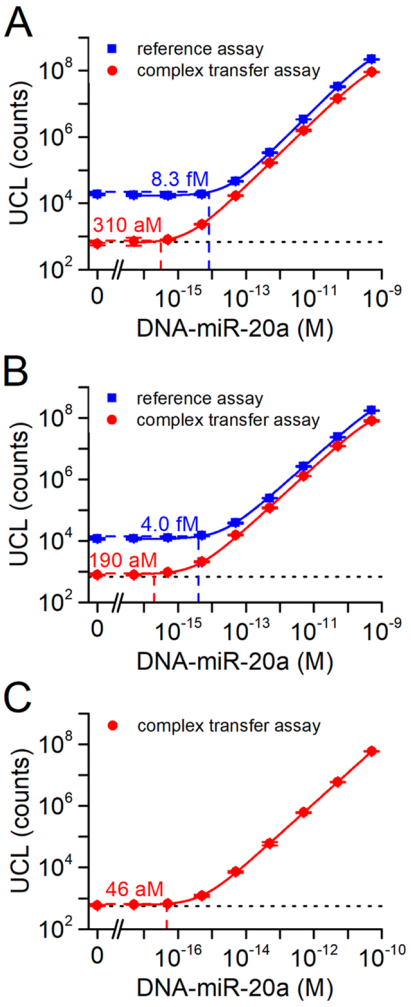

Figure 3. Standard curves of the complex transfer assay for the detection of DNA-miR-20a utilizing the MBs as the first capture surface (red circles) and the reference assay with direct capture on the second capture surface (blue squares) by using (A) 120 μL of sample volume per reaction with the assay buffer as the sample matrix, (B) 120 μL sample volume per reaction with EDTA plasma pool as a sample matrix, and (C) preconcentration from 600 μL of sample volume per reaction with the assay buffer as the sample matrix. Dashed lines indicate the LODs, and dotted lines show the instrument background. Error bars represent the standard deviations of three replicates (or eight replicates in case of zero calibrators).

molecules) for the hybridization complex transfer assay and 4.0 fM (290,000 molecules) for the reference assay (Figure 3B). The assay was able to detect similar target concentrations in undiluted plasma as in the buffer, and the LOD was 4 orders of magnitude lower than the reported miR-20a concentration in plasma.[38] This LOD indicates that the target can be detected directly in plasma without additional sample pretreatment. Generally, circulating miRNA concentrations are in the atto- to picomolar range.[39,40] Thus, the assay is likely to be almost universally applicable for the detection of miRNA by simply changing the sequences of the capture and tracer probes.

Using magnetic MBs as the solid phase in the first capture step has the additional benefit of enabling the collection of target molecules from a relatively large sample volume and concentrating them by doing the strand displacement reaction in a significantly smaller volume. The preconcentration step enables the detection of even lower target concentrations in the sample. Therefore, a 5-fold increase in the initial sample volume (600 μL) was used (Figure 3C), resulting in a 6.7-fold improvement in the LOD (46 aM, corresponding to 17,000 molecules). Compared to the reference assay in Figure 3A without complex transfer and preconcentration, the improvement was 180-fold.

As the sensitivity of the complex transfer assay was limited by the instrumental background noise and the detectability of the label, it is expected that the LOD could be further reduced by using larger UCNPs to increase their brightness or by changing the detection method. For example, only a small number of UCNPs bound to the surface are sufficient for a digital readout.[23,41] Additionally, the detectability of the signal could be improved by reducing the capture surface area in the second capture step to increase the label density.[25,42]

Some miRNAs differ by only a single nucleotide, making the ability to discriminate between minor sequence variations an essential feature of miRNA assays. To generate a signal in the complex transfer assay, the noncomplementary sequence has to cross-react with two capture probes sequentially, whereas in the reference assay, binding to one capture probe is enough. Therefore, the complex transfer assay was expected to have a lower cross-reactivity than the reference one. The cross-reactivities of MB-based complex transfer assay and reference assay were studied by using 0.5 pM DNA oligonucleotides, which contain minor variations in the sequence of the complementary target (Table S1). The luminescence signals were normalized to the complementary target signal; the normalized signal responses of each sequence are presented in Figure 4. The sequence with only a single nucleotide difference

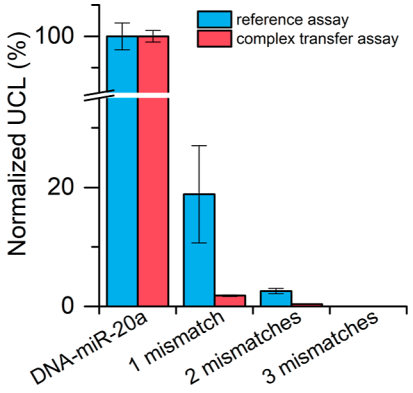

Figure 4. Cross-reactivity of the complex transfer assay (red) and the reference assay (blue) with sequences containing minor target sequence variations (0.5 pM; complete sequences are provided in Table S1). The luminescence signal responses are presented as percentage of the signal of the complementary target (DNA-miR-20a). The error bars represent the standard deviations of three replicate wells.

from the complementary target resulted in 1.8% and 19% cross-reactivity in complex transfer and reference assay, respectively. The sequence containing two mismatched nucleotides (DNA analogue of miR-20b) had 0.4% and 2.6% cross-reactivity in complex transfer and reference assay, respectively. Additionally, to study whether highly homologous sequences interfere with the quantitation of the target, samples containing various combinations of DNA analogues of miR-20a and miR-20b were prepared and analyzed with the complex transfer assay, and even 10-fold excess of nontarget

https://doi.org/10.1021/acs.analchem.4c05401
Anal. Chem. 2025, 97, 1775−1782

sequence did not interfere with the quantification of the target (Figure S7, Supporting Information). These results support the hypothesis that the complex transfer procedure significantly improves the assay specificity.

In our previous work, we developed a conventional sandwich hybridization assay on an MTP for the detection of the same sequence as in this work.[43] The direct assay principle was similar to that of the reference assay presented in this work. However, relatively long incubation times were necessary to compensate for the low UCNP label concentration employed to minimize nonspecific binding and, subsequently, the background signal. With a total assay time of approximately 4 h, the direct assay achieved an LOD of 0.73 fM. Although the complex transfer procedure in this work requires additional steps, it also allows for using 15-fold higher label concentration to improve binding kinetics without increasing the background signal, and the total assay time was decreased by approximately 1 h while achieving 16 times lower LOD.

Watanabe and Hashida[44] developed immunocomplex transfer assays with enzyme labels for three cytokines and compared them with similar assays without immunocomplex transfer. In their assay for TNF-α, the complex transfer decreased the specific signal by 65−71%, but due to the reduced nonspecific binding, the LOD improved 100-fold to 0.03 pg/mL, which corresponds to 1.7 fM monomeric TNF-α. Morrissey et al.[45] utilized a partly similar approach to improve the LOD of a radiolabel hybridization assay. Their approach used poly(dA)-tailed capture probes to enable the reversible capture of the target−probe complexes. The complexes were captured with polyT probes and eluted by the addition of a chaotropic salt. By repeating the capture and elution cycle three times, a 1000-fold improvement in the LOD and a detection limit of 40,000−100,000 molecules were achieved. In comparison, our complex transfer assay achieved an LOD of approximately 14,000 DNA target molecules.

Masterson et al.[46] reported localized surface plasmon resonance nanoplasmonic quantitation of microRNA-10b and microRNA-let7a, which are related to pancreatic ductal adenocarcinoma. They achieved an LOD of approximately 130 aM for both targets. Compared to the complex transfer assay reported here, their assay was carried out only in 10% plasma, and required overnight incubation. Ramshani et al.[47] developed a microfluidic sensor based on the electrokinetic membrane for free and extracellular vesicle-encapsulated microRNA miR-21 detection. This assay required only 20 μL of the sample, and the assay time was only 30 min, but the LOD of 1 pM was 4 orders of magnitude higher compared to our complex transfer assay. Majd et al.[48] developed a label-free hybridization assay using a molybdenum disulfide field-effect transistor biosensor for the detection of miRNA-155 as a breast cancer biomarker. They achieved LOD values of 0.03 fM in buffer and 0.1 fM in spiked human serum. However, the serum samples were 10-fold diluted with buffer before analysis, so the target concentration would have to be 10-fold higher in the untreated serum to be detectable. Wegman et al.[49] reported amplification-free analysis of multiple miRNAs by capillary electrophoresis with isotachophoresis preconcentration. Although the advantage of their approach is the possibility to detect several miRNAs in one experiment, their LOD was only 1 pM, which is about 4 orders of magnitude higher than the one obtained with our complex transfer assay.

CONCLUSIONS

A novel complex transfer technique was developed to eliminate the background signal from nonspecifically bound UCNPs in heterogeneous hybridization assays. The functionality of the method was demonstrated in the hybridization assay for the DNA analogue of miR-20a sequence as a model target, but the assay can be easily modified for the ultrasensitive detection of other nucleic acid biomarkers by changing the probe sequences. First, both capture steps were carried out in the MTP, achieving an LOD of 0.66 fM, which was 8.7 times lower compared to the LOD of the reference assay without the complex transfer. These results indicate that despite the unique optical properties of UCNPs, the nonspecific adsorption of labels to the detection surface is the biggest obstacle in reaching ultralow LODs. This limitation was overcome by our complex transfer approach, which eliminated the background and thus improved the LOD. Moreover, the additional steps combined with the MBs as the first detection surface enabled preconcentration of the target, which can be exploited to further improve the sensitivity. Using MBs as the first capture surface, LODs of 0.31 and 0.19 fM were achieved for buffer and EDTA plasma, respectively. These represent 27-fold and 21-fold improvements compared to the reference assay. A slightly lower LOD in the plasma proves the ability of the assay to be sensitive for the detection of nucleic acids in clinical samples without matrix interference. Additionally, using MBs as the first capture surface allowed sample preconcentration from a larger volume, resulting in an LOD of 46 aM. Furthermore, using two target-specific capture steps in the complex transfer assay improved discrimination between highly homologous sequences compared to the reference assay involving only a single capture step. The results indicate that the complex transfer assay is suitable for the direct detection of low-abundance circulating miRNA biomarkers, making it a powerful tool for cancer screening and early stage diagnostics.

ASSOCIATED CONTENT

Supporting Information

The Supporting Information is available free of charge at https://pubs.acs.org/doi/10.1021/acs.analchem.4c05401.

Information on oligonucleotide design and sequences of oligonucleotides, synthesis and surface modification of UCNP labels and their conjugation with oligonucleotide probes; information about plasma pool collection and in-house coating of MTPs with streptavidin; characterization of UCNP labels; and results from the optimization of the assay performance (PDF)

AUTHOR INFORMATION

Corresponding Author

Saara Kuusinen − *Department of Life Technologies/Biotechnology, Faculty of Technology, University of Turku, 20520 Turku, Finland;* orcid.org/0000-0003-4910-1905; Email: saevku@utu.fi

Authors

Jakub Máčala − *Department of Biochemistry, Faculty of Science, Masaryk University, 625 00 Brno, Czech Republic*

Satu Lahtinen − *Department of Life Technologies/Biotechnology, Faculty of Technology, University of Turku, 20520 Turku, Finland;* orcid.org/0000-0003-2816-7809

https://doi.org/10.1021/acs.analchem.4c05401
Anal. Chem. 2025, 97, 1775−1782

Hans H. Gorris − *Department of Biochemistry, Faculty of Science, Masaryk University, 625 00 Brno, Czech Republic;* orcid.org/0000-0003-1148-4293

Petr Skládal − *Department of Biochemistry, Faculty of Science, Masaryk University, 625 00 Brno, Czech Republic;* orcid.org/0000-0002-3868-5725

Zdeněk Farka − *Department of Biochemistry, Faculty of Science, Masaryk University, 625 00 Brno, Czech Republic;* orcid.org/0000-0002-6842-7081

Tero Soukka − *Department of Life Technologies/ Biotechnology, Faculty of Technology, University of Turku, 20520 Turku, Finland;* orcid.org/0000-0002-1144-6724

Complete contact information is available at: https://pubs.acs.org/10.1021/acs.analchem.4c05401

Author Contributions

[§]J.M. and S.K. contributed equally to this work.

Notes

The authors declare no competing financial interest.

■ ACKNOWLEDGMENTS

The authors thank Jaana Rosenberg from the University of Turku for synthesizing the UCNPs and Julian Brandmeier from the University of Regensburg for the surface modification of UCNPs. The work was supported by grant GA22-27580S from the Czech Science Foundation.

■ REFERENCES

(1) Li, M.; Yin, F.; Song, L.; Mao, X.; Li, F.; Fan, C.; Zuo, X.; Xia, Q. *Chem. Rev.* **2021**, *121* (17), 10469−10558.
(2) Valihrach, L.; Androvic, P.; Kubista, M. *Mol. Aspects Med.* **2020**, *72*, 100825.
(3) Qian, S.; Chen, Y.; Xu, X.; Peng, C.; Wang, X.; Wu, H.; Liu, Y.; Zhong, X.; Xu, J.; Wu, J. *Anal. Biochem.* **2022**, *643*, 114593.
(4) Kim, D.-J.; Linnstaedt, S.; Palma, J.; Park, J. C.; Ntrivalas, E.; Kwak-Kim, J. Y. H.; Gilman-Sachs, A.; Beaman, K.; Hastings, M. L.; Martin, J. N.; Duelli, D. M. *J. Mol. Diagn.* **2012**, *14* (1), 71−80.
(5) Koshiol, J.; Wang, E.; Zhao, Y.; Marincola, F.; Landi, M. T. *Cancer Epidemiol. Biomarkers Prev.* **2010**, *19* (4), 907−911.
(6) Li, W.; Ruan, K. *Anal. Bioanal. Chem.* **2009**, *394* (4), 1117−1124.
(7) Koscianska, E.; Starega-Roslan, J.; Sznajder, L. J.; Olejniczak, M.; Galka-Marciniak, P.; Krzyzosiak, W. J. *BMC Mol. Biol.* **2011**, *12* (1), 14.
(8) Liang, G.; Wang, H.; Shi, H.; Wang, H.; Zhu, M.; Jing, A.; Li, J.; Li, G. *J. Nanobiotechnol.* **2020**, *18* (1), 154.
(9) Wen, S.; Zhou, J.; Zheng, K.; Bednarkiewicz, A.; Liu, X.; Jin, D. *Nat. Commun.* **2018**, *9* (1), 2415.
(10) Hlaváček, A.; Farka, Z.; Mickert, M. J.; Kostiv, U.; Brandmeier, J. C.; Horák, D.; Skládal, P.; Foret, F.; Gorris, H. H. *Nat. Protoc.* **2022**, *17* (4), 1028−1072.
(11) Wu, S.; Han, G.; Milliron, D. J.; Aloni, S.; Altoe, V.; Talapin, D. V.; Cohen, B. E.; Schuck, P. J. *Proc. Natl. Acad. Sci. U.S.A.* **2009**, *106* (27), 10917−10921.
(12) Guan, L.; Peng, J.; Liu, T.; Huang, S.; Yang, Y.; Wang, X.; Hao, X. *Anal. Chem.* **2023**, *95* (48), 17708−17715.
(13) Wu, X.; Li, Y.; Yang, M. Y.; Mao, C. B. *Mater. Today Adv.* **2021**, *12*, 100163.
(14) Chen, C.; Hu, S.; Tian, L.; Qi, M.; Chang, Z.; Li, L.; Wang, L.; Dong, B. *Biosens. Bioelectron.* **2024**, *252*, 116135.
(15) Wang, J.; Hua, G.; Li, L.; Li, D.; Wang, F.; Wu, J.; Ye, Z.; Zhou, X.; Ye, S.; Yang, J.; Zhang, X.; Ren, L. *Analyst* **2020**, *145* (16), 5553−5562.
(16) Güven, E.; Duus, K.; Lydolph, M. C.; Jørgensen, C. S.; Laursen, I.; Houen, G. *J. Immunol. Methods* **2014**, *403* (1−2), 26−36.
(17) Lahtinen, S.; Lyytikäinen, A.; Sirkka, N.; Päkkilä, H.; Soukka, T. *Microchim. Acta* **2018**, *185* (4), 220.
(18) Hariri, A. A.; Newman, S. S.; Tan, S.; Mamerow, D.; Adams, A. M.; Maganzini, N.; Zhong, B. L.; Eisenstein, M.; Dunn, A. R.; Soh, H. T. *Nat. Commun.* **2022**, *13* (1), 5359.
(19) Buchwalow, I.; Samoilova, V.; Boecker, W.; Tiemann, M. *Sci. Rep.* **2011**, *1* (1), 28.
(20) Wauthier, L.; Plebani, M.; Favresse, J. *Clin. Chem. Lab. Med.* **2022**, *60* (6), 808−820.
(21) Mendez-Gonzalez, D.; Lahtinen, S.; Laurenti, M.; López-Cabarcos, E.; Rubio-Retama, J.; Soukka, T. *Anal. Chem.* **2018**, *90* (22), 13385−13392.
(22) Baltierra-Jasso, L. E.; Morten, M. J.; Laflör, L.; Quinn, S. D.; Magennis, S. W. *J. Am. Chem. Soc.* **2015**, *137* (51), 16020−16023.
(23) Brandmeier, J. C.; Raiko, K.; Farka, Z.; Peltomaa, R.; Mickert, M. J.; Hlaváček, A.; Skládal, P.; Soukka, T.; Gorris, H. H. *Adv. Healthcare Mater.* **2021**, *10* (18), 2100506.
(24) Chang, L.; Rissin, D. M.; Fournier, D. R.; Piech, T.; Patel, P. P.; Wilson, D. H.; Duffy, D. C. *J. Immunol. Methods* **2012**, *378* (1−2), 102−115.
(25) Ekins, R. P.; Chu, F. W. *Clin. Chem.* **1991**, *37* (11), 1955−1967.
(26) Shapoval, O.; Brandmeier, J. C.; Nahorniak, M.; Oleksa, V.; Makhneva, E.; Gorris, H. H.; Farka, Z.; Horák, D. *Talanta* **2022**, *244*, 123400.
(27) Nsubuga, A.; Sgarzi, M.; Zarschler, K.; Kubeil, M.; Hübner, R.; Steudtner, R.; Graham, B.; Joshi, T.; Stephan, H. *Dalton Trans.* **2018**, *47* (26), 8595−8604.
(28) Raiko, K.; Lyytikäinen, A.; Ekman, M.; Nokelainen, A.; Lahtinen, S.; Soukka, T. *Clin. Chim. Acta* **2021**, *523*, 380−385.
(29) Chen, H.; Wang, L.; Yeh, J.; Wu, X.; Cao, Z.; Wang, Y. A.; Zhang, M.; Yang, L.; Mao, H. *Biomaterials* **2010**, *31* (20), 5397−5407.
(30) Weng, Z.; Yu, H.; Luo, W.; Guo, Y.; Liu, Q.; Zhang, L.; Zhang, Z.; Wang, T.; Dai, L.; Zhou, X.; Han, X.; Wang, L.; Li, J.; Yang, Y.; Xie, G. *ACS Nano* **2022**, *16* (2), 3135−3144.
(31) Kohno, T.; Ishikawa, E.; Mitsukawa, T.; Matsukura, S. *J. Clin. Lab. Anal.* **1988**, *2* (4), 209−214.
(32) Kohno, T.; Mitsukawa, T.; Matsukura, S.; Tsunetoshi, Y.; Ishikawa, E. *J. Clin. Lab. Anal.* **1989**, *3* (3), 163−168.
(33) Gorris, H. H.; Soukka, T. *Anal. Chem.* **2022**, *94* (16), 6073−6083.
(34) Chheda, U.; Pradeepan, S.; Esposito, E.; Strezsak, S.; Fernandez-Delgado, O.; Kranz, J. *J. Pharm. Sci.* **2024**, *113* (2), 377−385.
(35) Soukka, T.; Kuningas, K.; Rantanen, T.; Haaslahti, V.; Lövgren, T. *J. Fluoresc.* **2005**, *15* (4), 513−528.
(36) Yakovchuk, P.; Protozanova, E.; Frank-Kamenetskii, M. D. *Nucleic Acids Res.* **2006**, *34* (2), 564−574.
(37) Ekins, R.; Chu, F.; Micallef, J. *J. Biolumin. Chemilumin.* **1989**, *4* (1), 59−78.
(38) Zhou, X.; Zhu, W.; Li, H.; Wen, W.; Cheng, W.; Wang, F.; Wu, Y.; Qi, L.; Fan, Y.; Chen, Y.; Ding, Y.; Xu, J.; Qian, J.; Huang, Z.; Wang, T.; Zhu, D.; Shu, Y.; Liu, P. *Sci. Rep.* **2015**, *5* (1), 11251.
(39) Ferracin, M.; Lupini, L.; Salamon, I.; Saccenti, E.; Zanzi, M. V.; Rocchi, A.; Da Ros, L.; Zagatti, B.; Musa, G.; Bassi, C.; Mangolini, A.; Cavallesco, G.; Frassoldati, A.; Volpato, S.; Carcoforo, P.; Hollingsworth, A. B.; Negrini, M. *Oncotarget* **2015**, *6* (16), 14545−14555.
(40) Mitchell, P. S.; Parkin, R. K.; Kroh, E. M.; Fritz, B. R.; Wyman, S. K.; Pogosova-Agadjanyan, E. L.; Peterson, A.; Noteboom, J.; O'Briant, K. C.; Allen, A.; Lin, D. W.; Urban, N.; Drescher, C. W.; Knudsen, B. S.; Stirewalt, D. L.; Gentleman, R.; Vessella, R. L.; Nelson, P. S.; Martin, D. B.; Tewari, M. *Proc. Natl. Acad. Sci. U.S.A.* **2008**, *105* (30), 10513−10518.
(41) Farka, Z.; Mickert, M. J.; Hlaváček, A.; Skládal, P.; Gorris, H. H. *Anal. Chem.* **2017**, *89* (21), 11825−11830.
(42) Christopoulos, T. K.; Lianidou, E. S.; Diamandis, E. P. *Clin. Chem.* **1990**, *36* (8), 1497−1502.

(43) Kuusinen, S.; Lahtinen, S.; Soukka, T. *Anal. Sens.* **2024**, *4* (4), No. e202400005.
(44) Watanabe, T.; Hashida, S. *J. Immunol. Methods* **2018**, *459*, 76−80.
(45) Morrissey, D. V.; Lombardo, M.; Eldredge, J. K.; Kearney, K. R.; Groody, E. P.; Collins, M. L. *Anal. Biochem.* **1989**, *181* (2), 345−359.
(46) Masterson, A. N.; Chowdhury, N. N.; Fang, Y.; Yip-Schneider, M. T.; Hati, S.; Gupta, P.; Cao, S.; Wu, H.; Schmidt, C. M.; Fishel, M. L.; Sardar, R. *ACS Sens.* **2023**, *8* (3), 1085−1100.
(47) Ramshani, Z.; Zhang, C.; Richards, K.; Chen, L.; Xu, G.; Stiles, B. L.; Hill, R.; Senapati, S.; Go, D. B.; Chang, H.-C. *Commun. Biol.* **2019**, *2* (1), 189.
(48) Majd, S. M.; Salimi, A.; Ghasemi, F. *Biosens. Bioelectron.* **2018**, *105*, 6−13.
(49) Wegman, D. W.; Ghasemi, F.; Khorshidi, A.; Yang, B. B.; Liu, S. K.; Yousef, G. M.; Krylov, S. N. *Anal. Chem.* **2015**, *87* (2), 1404−1410.

https://doi.org/10.1021/acs.analchem.4c05401
Anal. Chem. 2025, 97, 1775−1782